LA-UR-23-28517

Approved for public release; distribution is unlimited.

Title:	Contributions for ENDF/B-VIII.1 Paper
Author(s):	Neudecker, Denise; Casperson, Robert J.; Lovell, Amy Elizabeth; Gibson, Nathan Andrew; Marshall, W.J.; Parsons, Donald Kent; Talou, Patrick
Intended for:	Nuclear Data Sheets Report
Issued:	2023-07-26 (Draft)

Contributions for ENDF/B-VIII.1 Paper

D. Neudecker[a], R.J. Casperson[b], A. Lovell[a], N. Gibson[a], W.J. Marshall[c], K. Parsons[a], P. Talou[a]
[a]Los Alamos National Laboratory, Los Alamos, NM 87545, USA,
[b]Lawrence Livermore National Laboratory, Livermore, CA 94550, USA
[c]Oak Ridge National Laboratory, Oak Ridge, TN 37831, USA

July 25, 2023

1 Neutron Reaction Covariances

The covariance session ran three big, distinctive initiatives for this library release cycle: since the last release of the library:

- A concerted effort was made to deliver covariances for ENDF/B-VIII.1 earlier in the β-release phase than previously to allow for more stringent verification and validation. Also, CSEWG member institutions stood up new codes for better testing of covariances.
- Templates of expected measurement uncertainties were developed to aid evaluators and experimenters in estimating or providing more complete experimental uncertainties.
- A discussion and vote was held on whether CSEWG wants to provide a library of formally adjusted nuclear data mean values and covariances.

1.1 Improved Testing of Nuclear Data Covariances

It was discussed at WANDA2020 [RBB+20] that some issues were found by community and users in ENDF/B-VIII.0 covariances after their release. It was mentioned that one issue in testing ENDF/B-VIII.0 covariances was that they were provided by evaluators too late in the β-release phases that insufficient time for thorough testing was available.

Therefore, the executive committee requested that first nuclear data covariances should already be delivered for ENDF/B-VIII.1β_1 in February 2023—about half a year earlier than was the case for ENDF/B-VIII.0. This additional time allowed for more stringent testing with LANL's ENDFtk [HCMG20] and CovVal codes [Neu22], and ORNL's AMPX code [DW16] during the release phases. The LLNL covariance testing employed a combination of NJOY [MMB+17], empy tools from EMPIRE [HCC+07], and x4i [Bro].

The following verification and validation tests were performed on covariances:

1. Is the formatting correct and can the data be processed by codes such as NJOY and AMPX [MMB+17, DW16]?,
2. Are mathematical properties satisfied?
3. Are physics properties satisfied?

On item 2., we tested for symmetry, positive semi-definiteness, and if correlations were within $\pm$ 1, and all covariance constraints. The checks for semi-definiteness and correlations often implicitly test for the same thing–negative eigenvalues. Differences between the checks arise since different energy ranges are emphasized in each of the tests (absolute covariances versus relative covariances, and correlations). For example, a negative eigenvalue found in the relative covariances at energies where the associated cross section is very small will not be very significant in the absolute covariances. The covariance constraint tests check whether the zero-sum rule for MF=35 data is enforced [END12]. A related constraint (though not explicitly documented in [END12]) is whether the total MF=33 covariances are

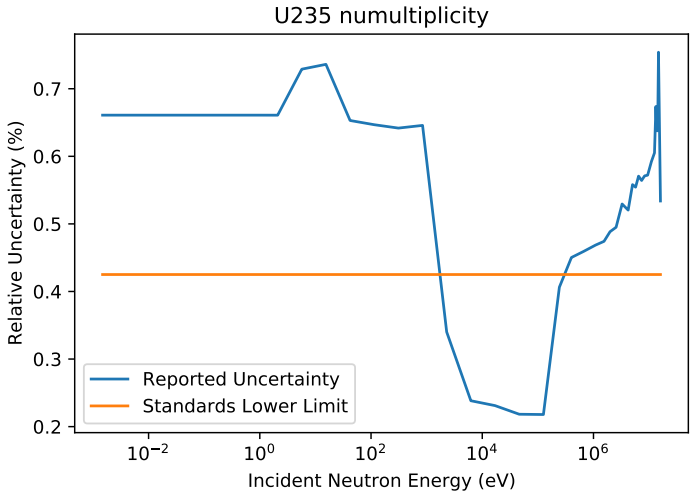

Figure 1: ^{235}U(n,f) $\overline{\nu}$ uncertainties for ENDF/B-VIII.1β1 are compared to standard, ^{252}Cf(sf) $\overline{\nu}_{\rm tot}$, uncertainties.

a sum of the partials covariances. For instance, MF=31, MT= 456 (covariances for the average prompt fission neutron multiplicity, $\overline{\nu}$) for ^{239}Pu failed for ENDF/B-VIII.1β_1 the test for positive definiteness. This covariance matrix was assembled from several pieces from three different institutes and a mistake had happened in the non-trivial assembly. This issue was found through testing for positive semi-definiteness as it led to medium-sized negative eigenvalues. It was corrected for ENDF/B-VIII.1β2.

On item 3., we test whether uncertainties are within reasonable limits, (e.g., no >100% uncertainties for mu-bar), uncertainties are larger than standard uncertainties of reaction most experimental data used to evaluate the observable are usually measured relative to, and uncertainties are realistic compared to template uncertainties [Neu21a, Smi21, NLMea23, LNCea23, Mat20, VHHea23, NDHea23, NCCea23, Mea23, Mat21, NST+20, NHT+18]. Also, the previous covariance session chair, D.L. Smith provided in Table 1 of Ref. [Smi21](repeated in Table I of Ref. [Neu21a]) reasonable lower bounds for evaluated uncertainties of specific nuclear data observables. Another test was employing upper and lower bounds obtained from the "Physical Uncertainty Bounds" [NWVS20] method for fission cross-section, PFNS and $\overline{\nu}$ uncertainties to cross-check whether evaluated uncertainties are realistic. While testing mathematical properties is often unambiguous in that the mathematical property is either satisfied or not, the tests of item 3. are less clear-cut but aim to provide some clues that uncertainties are either over or underestimated. It is then the job of the evaluator to judge, after being pointed to potential issues by these clues, whether uncertainties are indeed unrealistic given the evaluation input. One example is given with Fig. 1 that drew attention to the fact that ENDF/B-VIII.1β1 ^{235}U(n,f) $\overline{\nu}$ uncertainties were smaller than the current standard, ^{252}Cf(sf) $\overline{\nu}_{\rm tot}$, uncertainties from approximately 1–100 keV. This uncertainty lower than the standard is implausible as many $\overline{\nu}$ experimental data are measured relative to ^{252}Cf(sf) $\overline{\nu}_{\rm tot}$ and few data sets are available in that energy range. In fact, ^{235}U(n,f) $\overline{\nu}$ covariances were updated for thermal, resonance, and fast ranges but were carried over unchanged from ENDF/B-VIII.0 for 1–100 keV. However, the previous, much lower, ^{252}Cf(sf) $\overline{\nu}_{\rm tot}$ were applied for ENDF/B-VIII.0 ^{235}U(n,f) $\overline{\nu}$ covariances and it was missed to update the 1–100 keV range for ENDF/B-VIII.1β1 with the new standard uncertainties. This issue is being resolved for ENDF/B-VIII.1β2.

Additionally, visual comparisons were made between cross section confidence bands and EXFOR-data uncertainties [ODS+14], primarily looking for unjustifiably small or large uncertainties. For instance, ^{234}U(n,f) cross-section uncertainties improved significantly from ENDF/B-VIII.0 to ENDF/B-VIII.1β1: the evaluated uncertainties at 2 MeV incident neutron energy represent now better the existing experimental data. ^{234}U(n,n') cross-section uncertainties, on the other hand, were found to have a smaller uncertainty at 4 MeV than any of the major actinides despite an absence of data as can be seen from Fig. 2. Figure 3 shows a comparison of ^{234}U cross section uncertainties for ENDF/B-VIII.0 and ENDF/B-VIII.1β1.

Finally, the covariances provided in ENDF/B-VIII.1β1 were processed through AMPX and com-

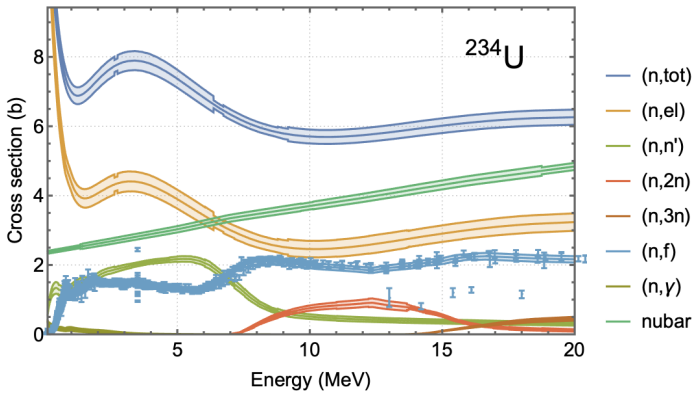

Figure 2: ^{234}U cross-section uncertainties for ENDF/B-VIII.1β1 are compared to EXFOR data to assess whether the uncertainties are reasonable given the spread in the experimental data.

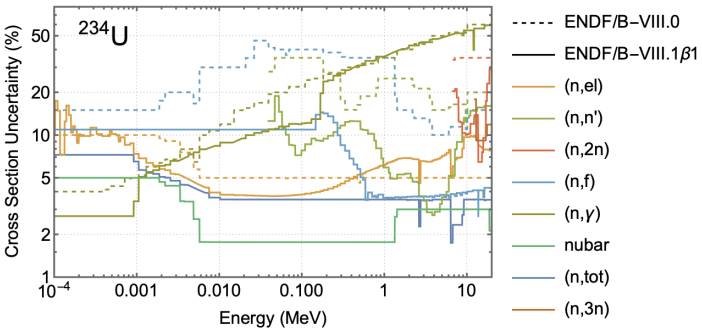

Figure 3: ^{234}U cross-section uncertainties for ENDF/B-VIII.0 and ENDF/B-VIII.1β1.

	# Cases	$\langle C/E \rangle$	$\langle$Exp. Unc.$\rangle$	St. Dev.(C/E)	VIII.0 σ	VIII.1 σ
HMF	50	1.00002	193	467	979	950
HST	52	0.999	494	615	652	792
IMF	13	1.00132	269	362	1027	1003
LCT	140	0.99874	195	162	603	737
LST	19	0.9992	318	283	824	944
MCT	49	0.99244	400	313	973	758
MST	10	0.99177	452	384	1323	1019
PMF	12	0.99902	207	133	1022	1038
PST	81	0.99927	497	429	1344	937

Table 1: Average simulated uncertainties, σ, on k_{eff} values of ICSBEP due to ENDF/B-VIII.0 and ENDF/B-VIII.1 covariances. All values except for # cases are in pcm.

bined with the SCALE 6.2 covariance library for any nuclides with no covariance data to generate a complete library for testing. This combined library was used to determine the estimated uncertainty in k_{eff} propagated from the nuclear data covariances for benchmarks in the VALID library maintained at ORNL [MR13] and for spent fuel in a hypothetical storage cask [Wag01]. The majority of the data-induced uncertainty in these systems comes from the major actinides, but the spent fuel system allows for testing the covariance data changes in major fission product nuclides typically credited in spent nuclear fuel (SNF) storage and transportation applications licensed by the US Nuclear Regulatory Commission [Bea20]. The results of the data-induced uncertainty for the benchmarks are summarized below in Table 1. The standard deviation of the C/E values within each benchmark category is compared to the average data-induced uncertainty using the SCALE covariance library based on ENDF/B-VIII.0 and the equivalent library based on ENDF/B-VIII.1 covariance data. In all 9 categories, including different uranium enrichments, plutonium, fast spectrum benchmarks, and thermal spectrum systems, the observed variability is significantly lower than the predicted variation based on the nuclear data covariance. The ENDF/B-VIII.1-based data has significantly lower overpredictions compared to the ENDF/B-VIII.0 data for thermal spectrum Pu-fueled systems. The overall uncertainty in these systems is reduced by 20–30%, with the change being driven by significant reductions in the ^{239}Pu PFNS, fission, and (n,γ) cross sections. The (n,γ) uncertainty dropped approximately 95%, which maybe require further evaluation in future releases. Unfortunately, the data-induced uncertainty increased for thermal spectrum U-fueled systems. This change was driven by increased uncertainty in ^{235}U $\overline{\nu}$. The reduction in ^{239}Pu uncertainty and increase in ^{235}U uncertainty for thermal systems will induce a shift in similarity metrics such as c_k for thermal SNF storage systems. C_k values will be increased for LEU experiments and reduced for mixed systems. Most major fission product evaluations remained unchanged, though ^{103}Rh uncertainty increased almost 30%. This represents the k_{eff} uncertainty from ^{103}Rh increasing from 21 pcm to 27 pcm in PWR fuel with a burnup of 40 GWd/MTU, so it is only a minor impact.

1.2 Templates of Expected Measurement Uncertainties

Templates of expected measurement uncertainties were established in Refs. [NLMea23, LNCea23, Mat20, VHHea23, NDHea23, NCCea23, Mea23, Mat21]. This effort was started after fission cross section templates [NST+20, NHT+18] and initial versions of total and capture templates were discussed at the fall CSEWG meeting of 2018. In spring 2019, a mini-CSEWG on that topic was held and the scope was extended to encompass prompt fission neutron spectra, average prompt and total fission neutron multiplicities, charged-particle cross sections, (n,xn) cross sections, and fission yield.

These provide listings of expected uncertainties for a specific measurement type related to one nuclear-data observables. For instance, transmission for total cross sections or absolute liquid-scintillator measurements for the average prompt fission neutron multiplicity. These listings can be used by experimenters as a check-list before the release of their data, or by evaluators to counter-check whether all pertinent uncertainties were provided for experiments chosen for their evaluation input database. Also, recommended values of many uncertainty sources are provided based on literature, EXFOR entries, and expert judgment from experimenters. These uncertainty values can be used as a last resort if they are not provided for a past experiments. These uncertainty values should only be used for

evaluations in the absence of other information to estimate the uncertainty source. Estimates of correlation coefficient between uncertainties of the same and different experiments for evaluation purposes are also given. The long-term goal of these templates is to provide better experimental uncertainties for evaluation purposes, be it either that experimenters use them as check-lists to provide data, or by evaluators to fill in missing uncertainties for their evaluation database. Ultimately, having better quantified experimental uncertainties for evaluation purpose will lead to more realistic evaluated uncertainties for nuclear data libraries.

1.3 Decision Process of CSEWG to not Provide Mathematically Adjusted Libraries for ENDF/B-VIII.1

Meeting records as far back as to the eighties of the last century show that CSEWG regularly had discussions on whether evaluated mean values and covariances should be formallyadjusted by the CSEWG community to trusted integral data. Formally adjusted means in this context that nuclear data mean values and covariances are updated with integral mean values and uncertainties via a mathematical algorithm such as generalized least squares. So far, this step has not been undertaken, but been left for the application user to do with integral experiments of their choice. However, ENDF/B nuclear data libraries do use information coming from integral data.

For instance, ENDF/B-VIII.0 nuclear data mean values were partially tweaked by hand or favorably selected to reproduce k_{eff} values of selected ICBSEP critical assemblies [ICS19], LLNL pulsed spheres [WAB+72], reaction rates, etc. [BCC+18]. Such changes were undertaken by computing integral data first with nuclear data obtained without integral information. Then a limited set of nuclear data, usually one or two observables, were changed by hand until one reached the desired agreement with integral data. Examples of such changes were documented for the thermal ^{239}Pu prompt fission neutron spectrum or for the ^{235}U average prompt fission neutron multiplicity in the resonance range [BCC+18]. Such changes are usually undertaken within the bounds of differential experimental data. In formal adjustment procedures, on the contrary, usually all nuclear data that are sensitive to the particular integral data are adjusted simultaneously.

Another important difference of by-hand tweaking and formal adjustment is that in the former case ENDF/B covariances remain unchanged. This leads to seemingly over-predicted k_{eff} uncertainties when one forward-propagates nuclear data covariances to simulated k_{eff} bounds and compares them to the spread in calculated over experimental k_{eff} values C/E [RBB+20]. As a consequence, some users don't use ENDF/B covariances because this tweaking renders covariances inconsistent with mean values.

It should also be mentioned that many of these changes and choices on nuclear data are not fully documented and neither are the benchmarks used for this by-hand tweaking and the reasoning for the choices. This lack of documentation also constitutes a problem for some user communities as it is unclear which k_{eff} benchmarks can be used for formal adjustment [RBB+20] while others are already incorporated in ENDF/B data. Of course, many of these tweaks are baked into ENDF/B libraries since generations of scientists. Removing them means re-doing major parts of ENDF/B.

Given this situation and frequent criticism by users [RBB+20], discussions on whether CSEWG should provide one true general-purpose library (i.e., without by-hand tweaking), and additional adjusted nuclear data libraries using formal mathematical algorithms came up regularly at CSEWG meetings. To reach a decision for what to do for ENDF/B-VIII.1, a vote on two questions regarding adjustment was held on August 19, 2021 at a mini-CSEWG session. These questions were:

1. Should CSEWG provide adjusted mean values and covariances *in addition* to our tweaked (general-purpose) library?

2. Should CSEWG provide tools or link to tools for adjustment on the NNDC homepage to help users do their own adjustment?

47 out of 55 participants cast a vote. Out of these, 68% voted against CSEWG providing adjusted mean values and covariances for ENDF/B-VIII.1. Instead, CSEWG will provide one general-purpose library with mean values tuned by hand to reproduce selected integral responses, while covariances remain unchanged. It is up to the users to do their own adjustment. A slim majority (51%) voted in favor to work towards providing links to tools for adjustment on the NNDC homepage.

Before the vote, the session was structured to enable participants to make an informed decision on these questions. There was a summary talk by the covariance session chair (D. Neudecker) from

a non-binding email survey on these questions within the covariance session before mini-CSEWG. This was followed by talks on currently in the U.S. available adjustment tools such as SCALE and Whisper [RWJ+11, BRA17]. Then, NNDC staff highlighted that they currently do not have the capabilities and bandwidth to store those adjusted libraries. Then two talks, one in favor and one opposed to adjustment, were provided, followed by a 20-minutes discussion and then the vote.

Concerns from people opposed and in favor of adjustment were documented in Ref. [Neu21b]. In general, many people showed interest in learning about potential weaknesses in adjustment results. However, a common concern in the discussion was that there are no tools applicable to integral responses catering to many subject areas, and that CSEWG is not yet ready to put out, and vet several adjusted libraries. Given these concerns, the following recommendations were given for the future:

- Results from adjustment and tool development should be discussed in the covariance session. The aim is to give recommendations to user how adjustment could be done and warn them about potential caveats. Also, evaluators could learn from adjustment results where nuclear data could be improved.
- If possible, evaluators should document some of their by-hand tweaks in ENDF/B-VIII.1 nuclear data along with the integral experiments used,
- Work should be undertaken in the future with the validation session to agree on what benchmarks/integral responses we use for tweaking. Integral responses used for tweaking should be carefully vetted.

2 ^{235}U

2.1 (n,f) Prompt Fission Neutron Spectrum

The ^{235}U PFNS at thermal energies was carried over from ENDF/B-VIII.0. PFNS at all other energies were re-evaluated as described in Ref. [NK22]. This evaluation builds on PFNS work included in ENDF/B-VIII.0 and documented in detail in Ref. [NTK+18]. The main difference is the inclusion of final high-precision ^{235}U PFNS measured by the Chi-Nu team of LANL and LLNL [KGD+22]. For ENDF/B-VIII.0, preliminary Chi-Nu PFNS were included for PFNS above incident neutron energies, $E_{\rm inc}$, of 5 MeV; these preliminary data were only going up to outgoing neutron energies, $E_{\rm out}$, of 2 MeV. Now, the final Chi-Nu data are included for $E_{\rm inc}$ = 2–10 MeV and up to $E_{\rm out}$ of 10 MeV. Previously available data sets were measured at a limited incident neutron energy range or had larger uncertainties.

The new evaluated PFNS shown in Figs. 4 (top) follow closely ENDF/B-VIII.0 for $E_{\rm inc} < 6$ MeV except for a small decrease of the PFNS for $E_{\rm out} > 7$ MeV which reflects Chi-Nu data's shape. This decrease leads to a modest reduction of Godiva, Flattop and BigTen $k_{\rm eff}$ values by 52(11), 40(13) and 31(13) pcm [NK22].

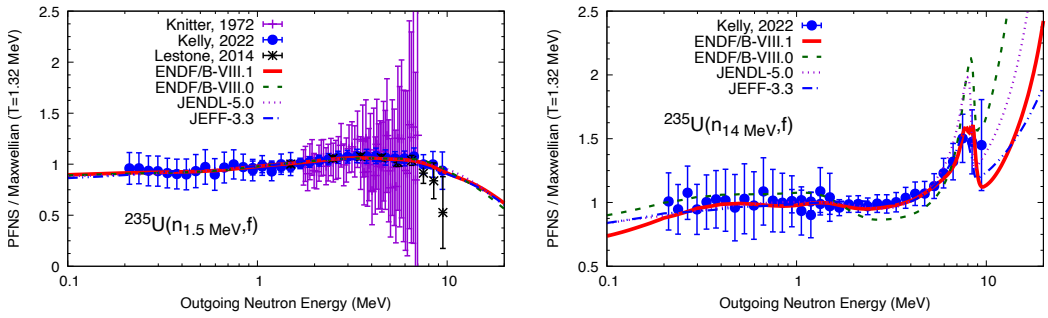

Figure 4: Experimental and evaluated ^{235}U PFNS for $E_{\rm inc}$=1.5 (top) and 14 MeV (bottom).

The changes from ENDF/B-VIIII.0 at higher $E_{\rm inc}$ are more pronounced as can be seen in the mean energy of the PFNS (Fig. 5) and individual PFNS (Fig. 4, bottom). The distinct change around $E_{\rm inc}$ of 14 MeV led to improvements in predicting ^{235}U LLNL pulsed sphere neutron leakage spectra in the valley after the peak, Figs. 10 and 11 in Ref. [NK22], and sown in Fig. 23.

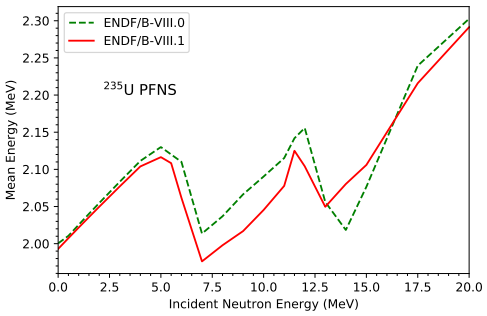

Figure 5: Evaluated ^{239}Pu PFNS mean energy.

E_{inc}	$\delta\langle E\rangle$ (keV)
Thermal	10
0.5–5	24
5–7	57
7–12	39
12–30	43

Table 2: The mean energy uncertainties, $\delta\langle E\rangle$, for the ^{235}U PFNS are listed per incident-neutron energy, E_{inc}.

Evaluated PFNS covariances are provided for five E_{inc} bins. Their mean energy uncertainties, $\delta\langle E\rangle$, are lowest in Table 2 at thermal and from 0.5–5 MeV, where most experimental data are available. In the E_{inc} bin spanning 0.5–5 MeV, the low uncertainties are driven by Chi-Nu (Kelly) and Lestone data at 1.5 MeV [KGD+22, LS14]. In fact, the too low uncertainties resulting from an evaluation with the Los Alamos model were increased to match Lestone uncertainties from E_{out} = 5–8 MeV which have the lowest ^{235}U PFNS uncertainties (Fig. 6).

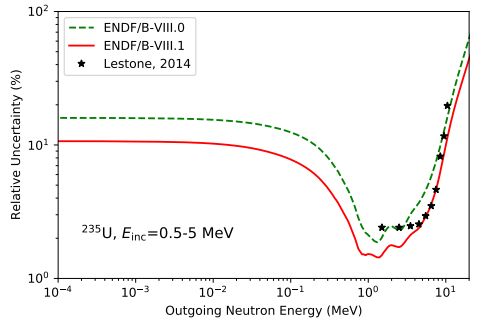

Figure 6: Evaluated ^{235}U PFNS uncertainties for E_{inc}=0.5–5 MeV.

2.2 (n,f) Fission $\overline{\nu}$

The neutron-induced average prompt fission neutron multiplicity, $\overline{\nu}$, for ^{235}U was re-evaluated from scratch for ENDF/B-VIII.0 [NLT21, LNT22]. Uncertainties for all experimental data were re-evaluated in detail using the literature of data sets as well as templates of expected $\overline{\nu}$ measurement uncertainties [NCCea23]. It was unclear what data were used for the previous evaluation, but all data currently in EXFOR were re-vistited. Also, similar to the ^{239}Pu $\overline{\nu}$ evaluation, the CGMF fission-event generator [TSJ+21] was used as model to evaluate $\overline{\nu}$. Including that model into the evaluation made it possible to employ evaluated model parameters to compute other fission quantities such as yields as a function of mass, the average total kinetic energy of fission fragments, etc. It was shown in Ref. [LNT22] that

most of these predicted fission quantities agree well with experimental data except for the PFNS—a known model deficiency that is being investigated. This combined new information led to changes from ENDF/B-VIII.0 (Fig. 7)—on the order of 0.5% up to 5 MeV. The changed $\overline{\nu}$ resulted originally in an increase in Godiva k_{eff} by 114(10) pcm. However, $\overline{\nu}$ was tweaked from 2.5–5.5 MeV where the model stiffness led to a departure from the evaluation with only experimental data [LNT22]. The tweaked $\overline{\nu}$ changes Godiva k_{eff} by 31(10) pcm.

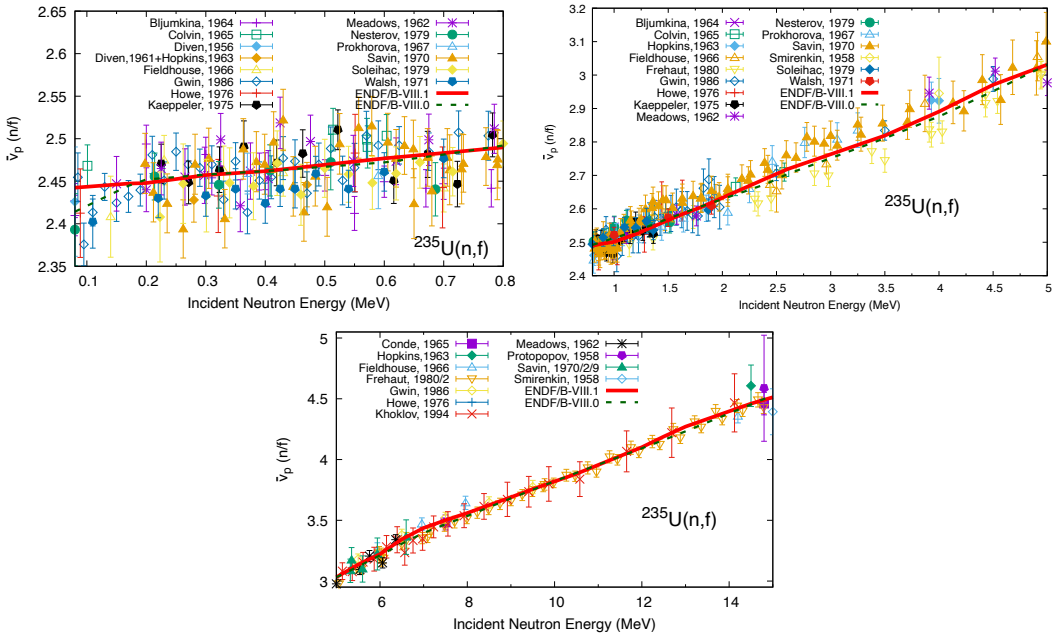

Figure 7: Experimental and evaluated ^{235}U $\overline{\nu}$.

The ENDF/B-VIII.1 evaluated uncertainties in Fig. 8 are distinctly larger above 80 keV due to the increased ^{252}Cf(sf) standards uncertainties (0.42%). The correlation matrix is strongly correlated due to the full correlation stemming from the dominant ^{252}Cf(sf) standards uncertainties. It is likely that this uncertainty will be revisited.

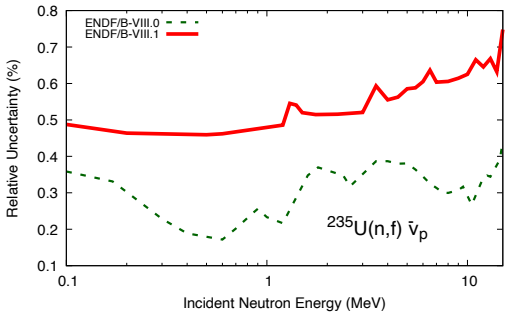

Figure 8: Evaluated ^{235}U $\overline{\nu}$ correlation matrix.

3 ^{238}U

3.1 (n,f) Fission $\overline{\nu}$

4 ^{239}Pu

4.1 (n,f) Prompt Fission Neutron Spectrum

The ^{239}Pu PFNS at thermal energies

PFNS at all other energies were re-evaluated as described in Ref. [NLK+23, NKM22] and builds on PFNS work included in ENDF/B-VIII.0 [NTK+18]. The main difference is the inclusion of high-precision ^{239}Pu PFNS measured by the CEA and Chi-Nu teams [KDO+20, KMT+21, MTL+20] at Lestone data at $E_{\rm inc}$=2 MeV [LS14]. The evaluated PFNS differ distinctly at all incident-neutron energies from ENDF/B-VIII.0 as can be seen in the change of mean energy in Fig. 9. However, in changing distinctly they follow more closely the new experimental data sets as can be seen for $E_{\rm inc}$=1.5 and 14 MeV in Fig. 10.

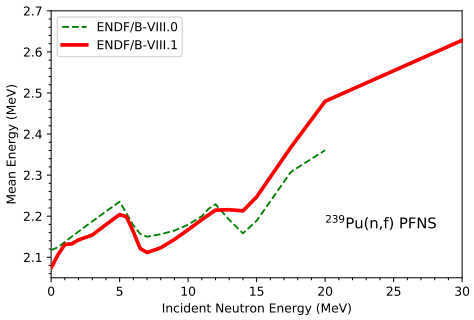

Figure 9: Evaluated ^{239}Pu PFNS mean energy.

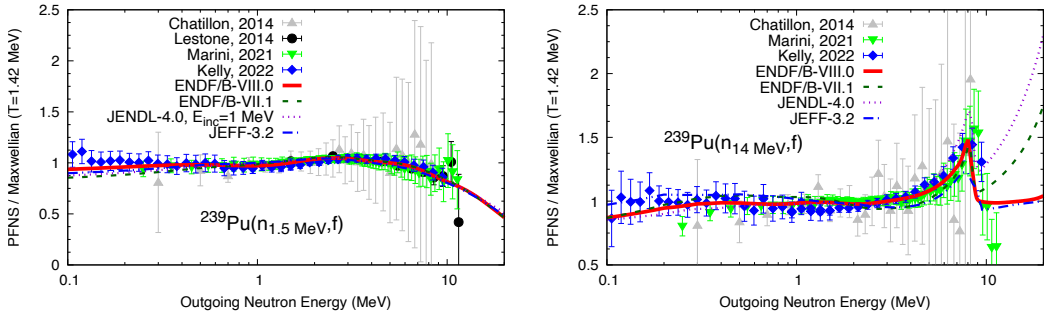

Figure 10: Experimental and evaluated ^{239}Pu PFNS for $E_{\rm inc}$=1.5 (top) and 14 MeV (bottom).

This distinct change in the PFNS led to a significant decrease in Jezbel and Flattop-Pu $k_{\rm eff}$ values by 128(1) and 114(1) pcm [NLK+23, NKM22]. It was counter-balanced by other changes in ^{239}Pu, such as in the average prompt fission neutron multiplicity. The changes in the prediction of the Pu LLNL pulsed-sphere neutron-leakage spectra were modest [NLK+23, NKM22].

Evaluated PFNS covariances are provided for seven $E_{\rm inc}$ bins. Their mean energy uncertainties, $\delta\langle E\rangle$, are lowest in Table 3 at thermal and from 0.75–3 MeV, where most experimental data are available. In the $E_{\rm inc}$ bin spanning 0.75–3 MeV (Fig. 11) , the low uncertainties are driven by Marini, Chi-Nu (Kelly) and Lestone data at 1.5 MeV [KDO+20, KMT+21, MTL+20, LS14].

E_{inc}	$\delta\langle E\rangle$ (keV)
Thermal	16
0.25–0.75	37
0.75–3	15
3–5	33
5–6.5	33
6.5–13	34
13–30	40

Table 3: The mean energy uncertainties, $\delta\langle E\rangle$, for the ^{239}Pu PFNS are listed per incident-neutron energy, E_{inc}.

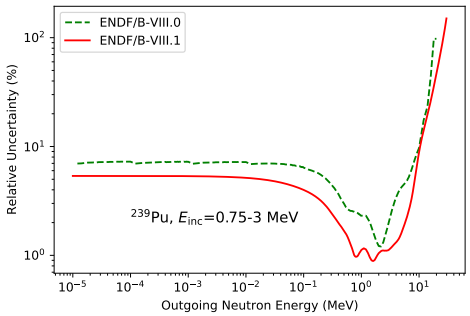

Figure 11: Evaluated ^{239}Pu PFNS uncertainties for E_{inc}=0.75–3 MeV.

4.2 (n,f) Fission $\overline{\nu}$

The neutron-induced average prompt fission neutron multiplicity, $\overline{\nu}$, for ^{239}Pu was re-evaluated from scratch for ENDF/B-VIII.0 [NLK+23, NLT21]. Uncertainties for all experimental data were re-evaluated in detail using the literature of data sets as well as templates of expected $\overline{\nu}$ measurement uncertainties [NCCea23]. Also, the very recent high-precision data by Marini et al. [MTN+21] were included in the new evaluation. Also, for the very first time, the CGMF fission-event generator [TSJ+21] was used as model to evaluate $\overline{\nu}$. Including that model into the evaluation made it possible to employ evaluated model parameters to compute other fission quantities such as yields as a function of mass, the average total kinetic energy of fission fragments, etc. It was shown in Ref. [NLK+23] that most of these predicted fission quantities agree well with experimental data except for the PFNS—a known model deficiency that is being investigated. This combined new information led to distinct changes from ENDF/B-VIII.0 in Fig. 12. The changed $\overline{\nu}$ resulted in an increase in Jezebel k_{eff} by 139(1) pcm that was counter-balanced by the new ^{239}Pu PFNS.

The ENDF/B-VIII.1 evaluated uncertainties in Fig. 13 are larger from 80 keV to approximately 2 MeV due to the increased ^{252}Cf(sf) standards uncertainties (0.42%), and smaller below 2 MeV due to Marini et al. high-precision data. The correlation matrix in Fig. 14 is strongly correlated due to the full correlation stemming from the dominant ^{252}Cf(sf) standards uncertainties. It is likely that this uncertainty will be revisited.

4.3 (n,f) Fission Cross Section

For ENDF/B-VIII.0, neutron-induced fission cross sections for ^{239}Pu were reported by the Neutron Data Standards committee [CPC+18] with covariances enlarged by a fully-correlated USU (unrecognized sources of uncertainties [CBC+20]) component. This USU uncertainty should account for known but missing uncertainty sources and correlations in the input to the evaluation as well as unknown uncertainties. While the latter can only be assessed by the spread of data among experiments employing different measurement techniques, the former were tackled by creating templates of expected fission cross-section uncertainties and applying them to ^{239}Pu(n,f) cross-section data in the database [NST+20, NHT+18]. In addition to that, fissionTPC ^{238}U/^{235}U and ^{239}Pu/^{235}U [SAB+21] neutron induced fission cross-section shape ratios were included into the evaluation [NPS21]. The final

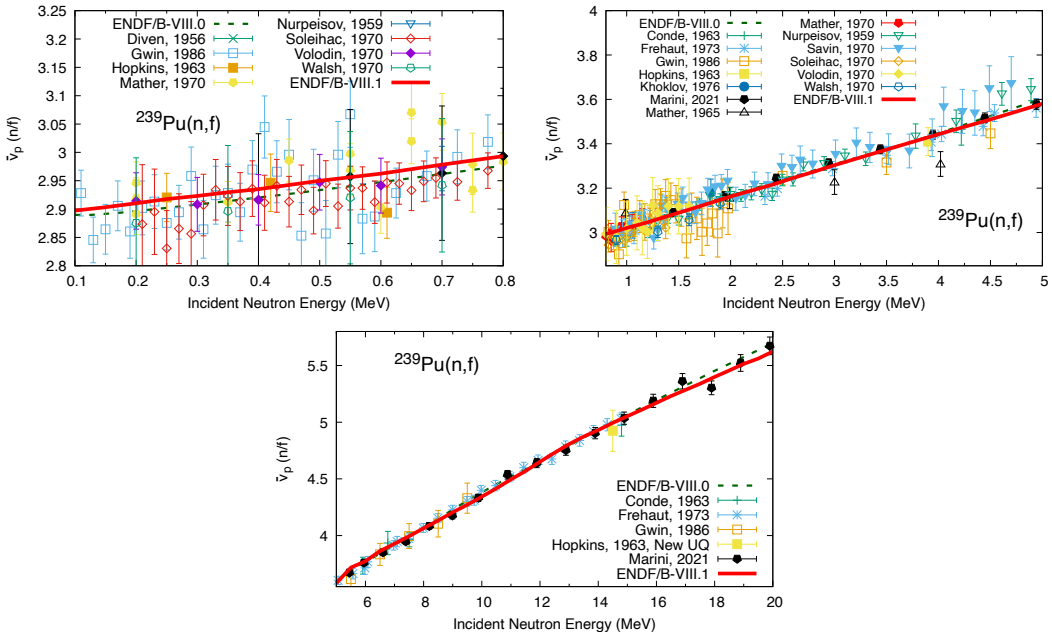

Figure 12: Experimental and evaluated ^{239}Pu $\overline{\nu}$.

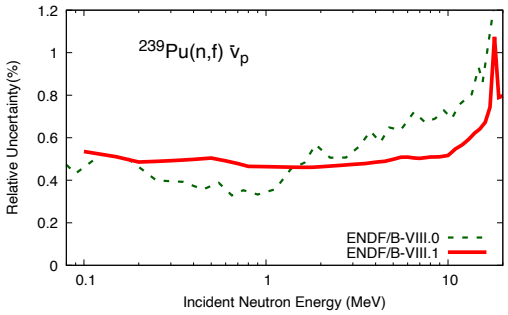

Figure 13: Evaluated ^{239}Pu $\overline{\nu}$ correlation matrix.

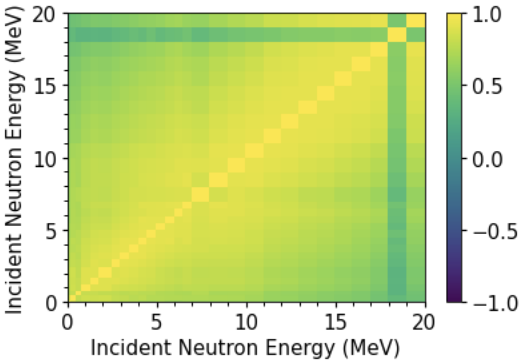

Figure 14: Evaluated ^{239}Pu $\overline{\nu}$ correlation matrix.

^{239}Pu(n,f) cross section cross section implemented in ENDF/B-VIII.1 was presented in Ref. [NLK+23] and is compared to fissionTPC data in Fig. 15 as a ratio to ^{235}U(n,f) cross sections. Inclusion of the high-precision fissionTPC data reduced the cross section above 10 MeV. In this energy region, discrepant data sets led to questions on the shape of the cross section [CPC+18]; potential biases were suspected in quantifying the detector efficiency, especially, the effect of angular distribution on the

efficiency. FissionTPC data were measured with a time-projection chamber, another type of fission detector than the discrepant data used. This detector has a more fine-grained view of the angular distribution of fission fragments [SAB+21]. Hence, these new data lead to more trust in the new shape of the fission cross section at higher incident-neutron energies.

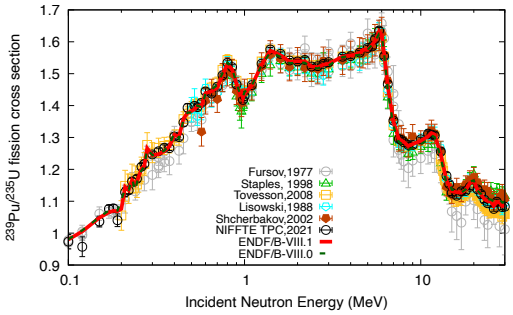

Figure 15: Evaluated ^{239}Pu/^{235}U cross section ratios compared to selected experimental data.

Finally, work was done to update the USU uncertainty component to have energy-dependent correlations rather than being fully correlated. This work was necessary as adjustment with the ^{239}Pu(n,f) ENDF/B-VIII.0 covariances with respect to Pu LLNL pulsed-spheres neutron-leakage spectra resulted in adjusting the fission cross sections with a nearly constant percentage factor down to a few 100 keV [NGA+23]. However, nearly the same percentage adjustments down to a few 100 keV is unrealistic as the Pu pulsed sphere is mostly sensitive to these data from 12–15 MeV [NCC+21] and multiple-chance fission effects should weaken the impact of adjustment considerably below 5 MeV.

5 Validation with LLNL Pulsed Spheres

LLNL pulsed-spheres neutron-leakage spectra provide neutron spectra over time of flight pulsed by a 14-MeV neutron source in the center of the sphere [WAB+72]. They allow us to validate nuclear data from 15 MeV down to several MeV dependent on the thickness and the level scheme of the nuclei at hand [NCC+21, ACC+22]. Below validation results with ENDF/B-VIII.0 and ENDF/B-VIII.1β1 are given. Also, hints are provided how predictions of neutron-leakage spectra can be improved by nuclear-data changes based on sensitivity profiles computed as part of the LANL EUCLID LDRD-DR project [NCC+21, ACC+22].

^{6}Li LLNL pulsed-sphere neutron-leakage spectra change distinctly in Fig. 16 when simulated with ENDF/B-VIII.0 and ENDF/B-VIII.1β1. The spheres are thin (0.5 mean free path and 1.6 mean free path); so little multiple scattering of neutrons will happen and most neutrons will be induced in the sphere by the incident-neutron beam with energies of 12–15 MeV. In this energy range, one major change happened for the ^{6}Li(n,n')dα cross sections; the reaction was changed from the laboratory to the center-of-mass-frame. system. To be clear, both evaluations are leading to large biases in simulating pulsed-sphere spectra. While the new evaluation get closer at later times, it produces structures in the simulated data close to the peak that are not supported by experimental data. One could study changing MF = $\{3, 4\}$ MT=53 for better predicting ^{6}Li LLNL pulsed-sphere neutron-leakage spectra.

The ^{9}Be LLNL pulsed-sphere neutron-leakage spectra in Fig. 17 are described worse around the elastic peak with ENDF/B-VIII.1β1 compared to ENDF/B-VIII.0. One should, however, keep in mind that the pulsed spheres are not formal benchmarks and they are more uncertain than k_{eff} values. All spheres are less in size than one mean free path. Thus, one should investigate nuclear data for incident-neutron energies of 12–15 MeV to increase the predictive power of ^{9}Be nuclear data for simulating ^{9}Be pulsed spheres. One could investigate (n,2n) cross sections and angular distributions, elastic angular distributions, or the new (n,inl) cross sections and angular distribution. The latter likely only have a small effect on the simulation of ^{9}Be pulsed spheres.

There are only small changes observed in the simulations of pulsed spheres containing ^{16}O to a non-negligible amount (Light water in Fig. 20, "pure" ^{16}O and heavy water in Fig. 19 and concrete in Fig. 18) if one uses ENDF/B-VIII.0 and ENDF/B-VIII.1β1 nuclear data. If one would like to improve

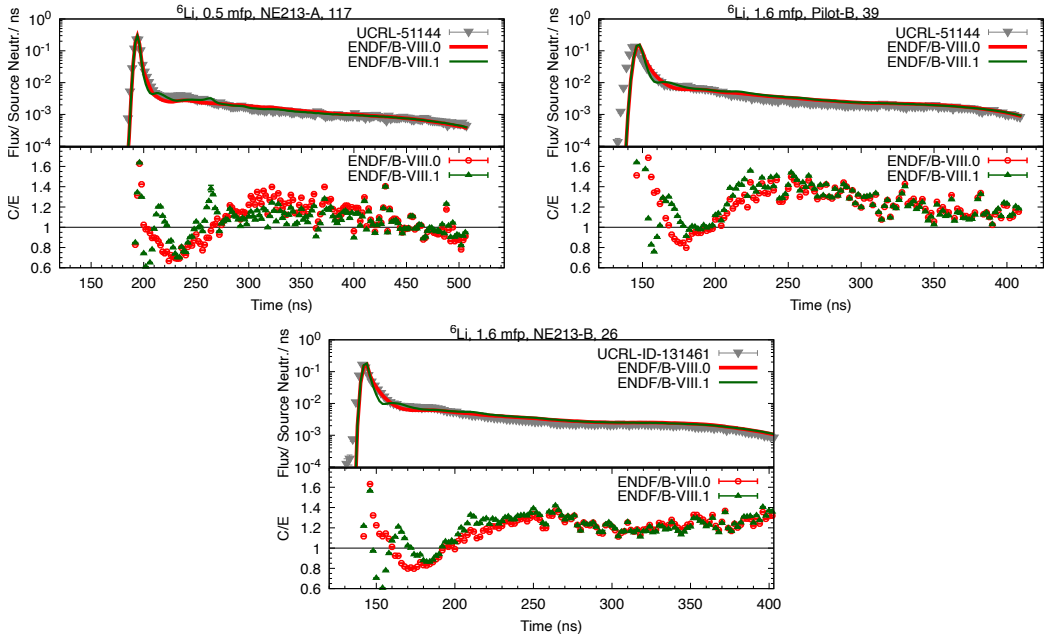

Figure 16: LLNL pulsed-sphere neutron-leakage spectra simulated with ENDF/B-VIII.0 and ENDF/B-VIII.1β1 for ^{6}Li compared to experimental data.

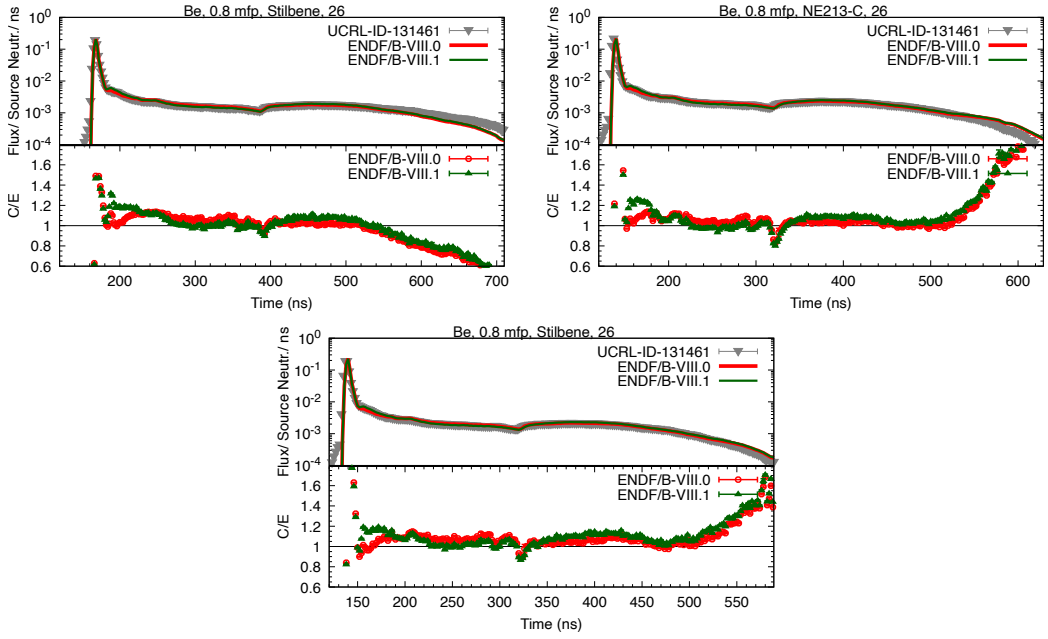

Figure 17: LLNL pulsed-sphere neutron-leakage spectra simulated with ENDF/B-VIII.0 and ENDF/B-VIII.1β1 for ^{8}Be compared to experimental data.

agreement of simulations right after the peak, one could investigate MF=4, MT2, and MF=$\{3,4\}$, MT=52, as these ^{16}O observables matter most in the simulations of the spheres shown.

Small improvements can be observed in simulations of Teflon LLNL pulsed-sphere neutron-leakage spectra in Fig. 21 if ENDF/B-VIII.1β1 nuclear data are used. The overall agreement is poor which could be either due to carbon or ^{19}F nuclear data given the fact that the predictions of carbon pulsed spheres is also poor. If one would like to try to improve predictions of Teflon pulsed-sphere spectra via ^{19}F nuclear data, one could investigate MF=4, MT2 and MF=$\{3,4\}$, MT=51,55 nuclear data.

The updates in Fe ENDF/B-VIII.1β1 nuclear data compared to ENF/B-VIII.0 led to only small

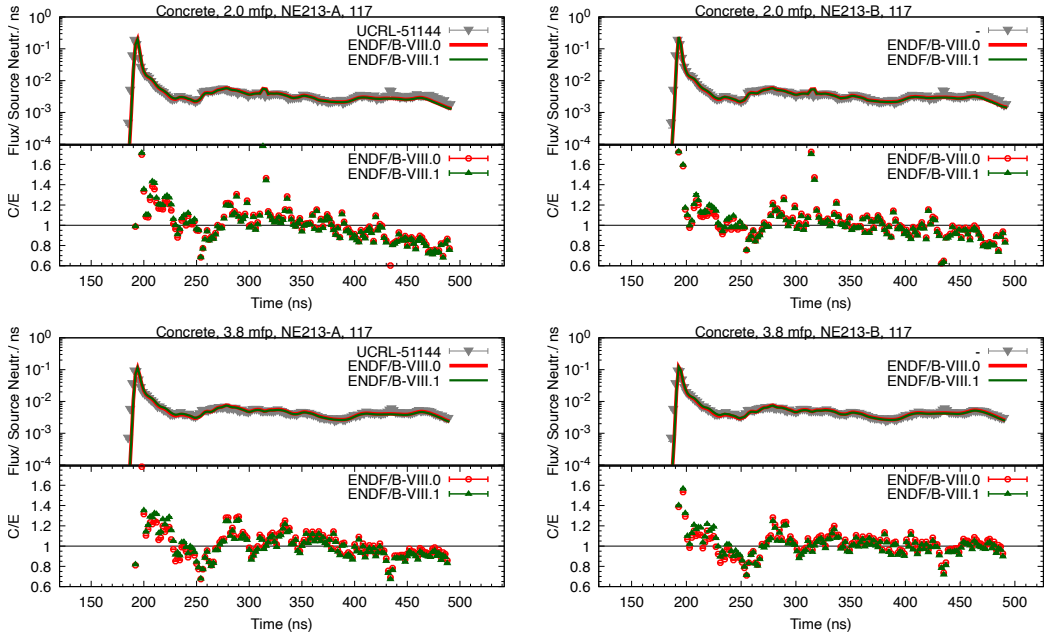

Figure 18: LLNL pulsed-sphere neutron-leakage spectra simulated with ENDF/B-VIII.0 and ENDF/B-VIII.1β1 for concrete compared to experimental data.

changes in the simulated Fe LLNL pulsed-sphere neutron-leakage spectra. It can be seen in Fig. 22 that the changes are a bit larger for thicker spheres than thinner ones. The thicker the sphere, the more multiple scattering of neutrons happens and one uses lower-energy nuclear data (4–10 MeV) for the spectra's simulations. Hence, changes inelastic data (MF=$\{3, 4, 6\}$) is likely an important contributor to differences in simulated spectra. If one would like to improve agreement between simulations and experiments at later times, one could investigate at MF=6, MT=91 iron nuclear data.

The ^{235}U LLNL pulsed-sphere neutron-leakage spectra in Fig. 23 are noticeably better described with ENDF/B-VIII.1β1 data than ENDF/B-VIII.0 in the valley after the elastic peak. This improved agreement has already been observed for ENDF/B-VIII.1β0. It was attributed to the new ^{235}U PFNS evaluation that changed significantly from 12–15 MeV due to inclusion of high-precision Chi-Nu experimental data [NK22].

Large changes can be observed for ^{239}Pu LLNL pulsed-sphere neutron-leakage spectra in Fig. 24 among predictions using four different evaluations:

- ENDF/B-VIII.0,
- ENDF/B-VIII.1β0 from the INDEN project,
- A LANL Oct. 2022 file,
- ENDF/B-VIII.1β1 that includes (n,2n) and (n,gamma) reaction cross sections from the INDEN ENDF/B-VIII.1β0 file, but also (n,inl) and (n,el) cross sections from the LANL October 2022 file. The fission-source term is the same across all files except ENDF/B-VIII.0.

The main difference between the INDEN and ENDF/B-VIII.1β1 simulation is caused by LANL's file (n,inl) and (n,el) cross sections and angular distributions. INDEN performs better, but the pulsed spheres are not accurate enough to make a firm enough statement which nuclear data is closer to truth.

Negligible changes were observed between ^{7}Li, ^{12,13}C, Pb and ^{238}U LLNL pulsed-sphere neutron-leakage spectra simulated with ENDF/B-VIII.0 and ENDF/B-VIII.1β1 despite changes in the nuclear data.

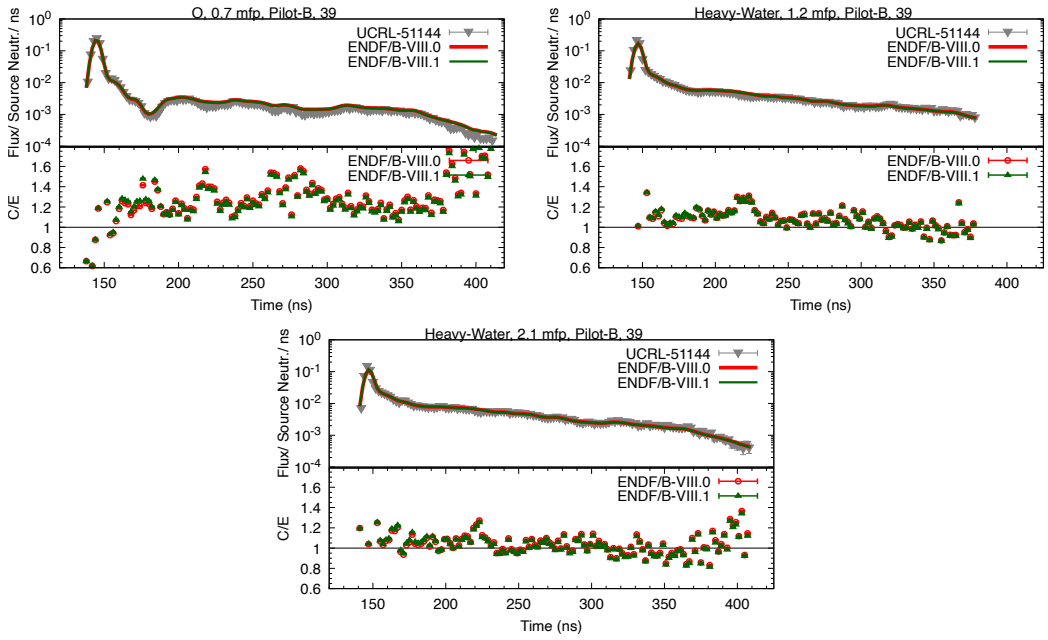

Figure 19: LLNL pulsed-sphere neutron-leakage spectra simulated with ENDF/B-VIII.0 and ENDF/B-VIII.1β1 for ^{16}O and heavy water compared to experimental data.

Acknowledgments

Research reported in this publication was partially supported by the U.S. Department of Energy LDRD program at Los Alamos National Laboratory. We gratefully acknowledge partial support of the Advanced Simulation and Computing program at LANL and the DOE Nuclear Criticality Safety Program, funded and managed by NNSA for the DOE. This work was supported by the US Department of Energy through the Los Alamos National Laboratory. Los Alamos National Laboratory is operated by Triad National Security, LLC, for the National Nuclear Security Administration of the US Department of Energy under Contract No. 89233218CNA000001.

References

[ACC+22] J. Alwin, A.R. Clark, T. Cutler, M.J. Grosskopf, W. Haeck, M.W. Herman, J. Hutchinson, N. Kleedtke, J. Lamproe, R.C. Little, I. Michaud, D. Neudecker, M.E. Rising, T. Smith, N. Thompson, and S.A. Vander Wiel. Euclid sensitivity database. Technical Report LA-UR-22-21534, Los Alamos National Laboratory, 2022.

[BCC+18] D. A. Brown, M. B. Chadwick, R. Capote, A. C. Kahler, A. Trkov, M. W. Herman, A. A. Sonzogni, Y. Danon, A. D. Carlson, M. Dunn, D. L. Smith, G. M. Hale, G. Arbanas, R. Arcilla, C. R. Bates, B. Beck, B. Becker, F. Brown, R. J. Casperson, J. Conlin, D. E. Cullen, M. A. Descalle, R. Firestone, T. Gaines, K. H. Guber, A. I. Hawari, J. Holmes, T. D. Johnson, T. Kawano, B. C. Kiedrowski, A. J. Koning, S. Kopecky, L. Leal, J. P. Lestone, C. Lubitz, J. I. Márquez Damián, C. M. Mattoon, E. A. McCutchan, S. Mughabghab, P. Navratil, D. Neudecker, G. P. A. Nobre, G. Noguere, M. Paris, M. T. Pigni, A. J. Plompen, B. Pritychenko, V. G. Pronyaev, D. Roubtsov, D. Rochman, P. Romano, P. Schillebeeckx, S. Simakov, M. Sin, I. Sirakov, B. Sleaford, V. Sobes, E. S. Soukhovitskii, I. Stetcu, P. Talou, I. Thompson, S. van der Marck, L. Welser-Sherrill, D. Wiarda, M. White, J. L. Wormald, R. Q. Wright, M. Zerkle, G. Žerovnik, and Y. Zhu. Endf/b-viii.0: The 8th major release of the nuclear reaction data library with cielo-project cross sections, new standards and thermal scattering data. *Nuclear Data Sheets*, 148:1 – 142, 2018.

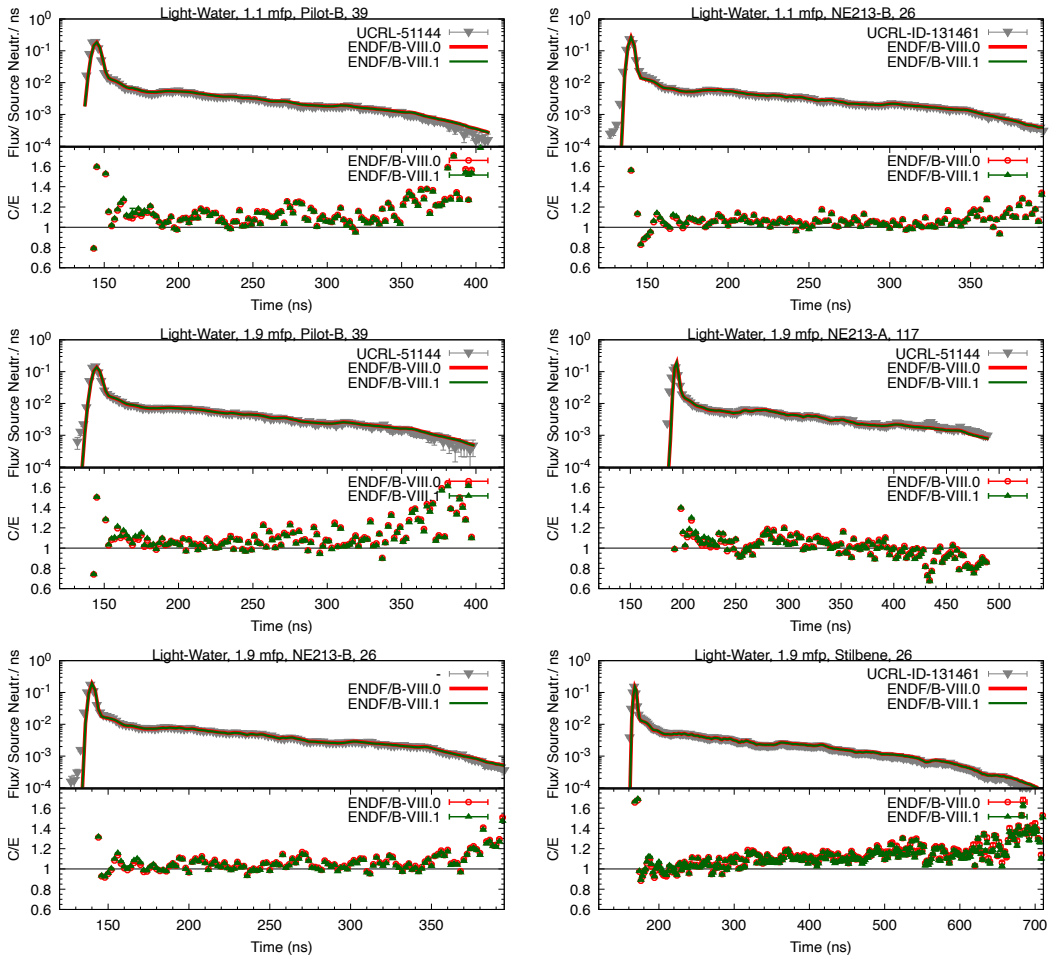

Figure 20: LLNL pulsed-sphere neutron-leakage spectra simulated with ENDF/B-VIII.0 and ENDF/B-VIII.1β1 for light water compared to experimental data.

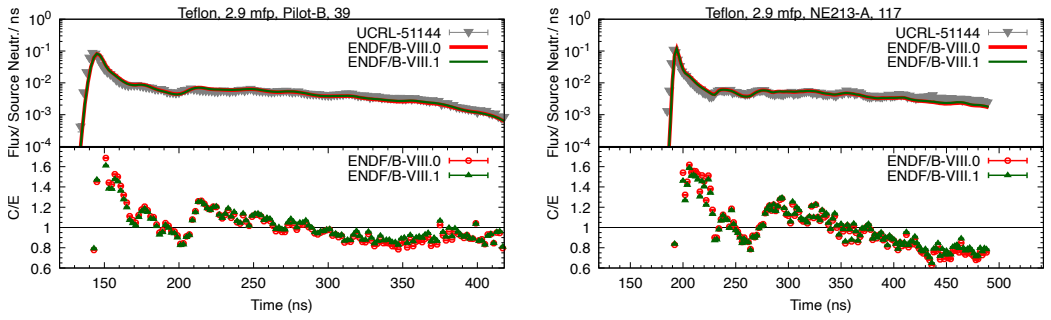

Figure 21: LLNL pulsed-sphere neutron-leakage spectra simulated with ENDF/B-VIII.0 and ENDF/B-VIII.1β1 for teflon compared to experimental data.

[Bea20] Joseph Borowski and et al. Standard review plan for transportation packages for spent fuel and radioactive material: Final report. Technical Report NUREG-2216, US Nuclear Regulatory Commission, Washing, DC, 2020.

[BRA17] F.B. Brown, M.E. Rising, and J.L. Alwin. User manual for whisper-1.1. Technical Report LA-UR-17-20567, Los Alamos National Laboratory, 2017.

[Bro] D. Brown, (2011), x4i: the EXFOR interface, https://github.com/brown170/x4i.

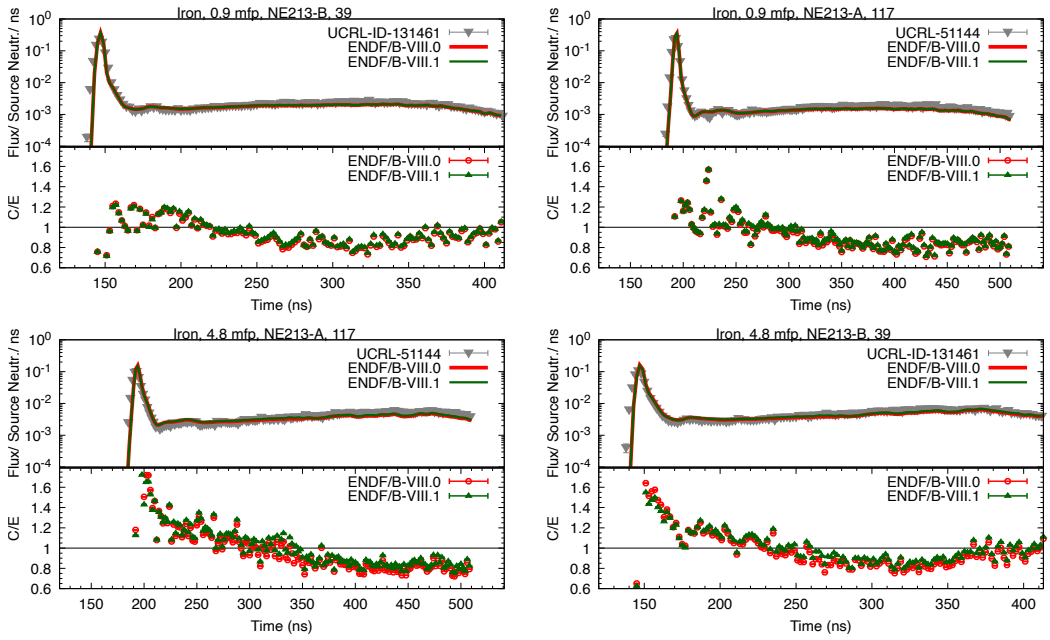

Figure 22: LLNL pulsed-sphere neutron-leakage spectra simulated with ENDF/B-VIII.0 and ENDF/B-VIII.1β1 for teflon compared to experimental data.

[CBC+20] R. Capote, S. Badikov, A.D. Carlson, I. Duran, F. Gunsing, D. Neudecker, V.G. Pronyaev, P. Schillebeeckx, G. Schnabel, D.L. Smith, and A. Wallner. Unrecognized sources of uncertainties (usu) in experimental nuclear data. *Nuclear Data Sheets*, 163:191–227, 2020.

[CPC+18] A.D. Carlson, V.G. Pronyaev, R. Capote, G.M. Hale, Z.-P. Chen, I. Duran, F.-J. Hambsch, S. Kunieda, W. Mannhart, B. Marcinkevicius, R.O. Nelson, D. Neudecker, G. Noguere, M. Paris, S.P. Simakov, P. Schillebeeckx, D.L. Smith, X. Tao, A. Trkov, A. Wallner, and W. Wang. Evaluation of the neutron data standards. *Nuclear Data Sheets*, 148:143–188, 2018. Special Issue on Nuclear Reaction Data.

[DW16] et al. D. Wiarda. AMPX-6: A Modular Code System for Processing ENDF/B. Technical Report ORNL/TM-2016/43, Oak Ridge National Laboratory, 2016. Available from Radiation Safety Information Computational Center as CCC-834.

[END12] ENDF-6 formats manual. Technical Report BNL-90365-2009 Rev. 2, Brookhaven National Laboratory, 2012.

[HCC+07] M. Herman, R. Capote, B.V. Carlson, P. Obložinský, M. Sin, A. Trkov, H. Wienke, and V. Zerkin. EMPIRE: Nuclear reaction model code system for data evaluation. *Nucl. Data Sheets*, 108:2655, 2007.

[HCMG20] W. Haeck, J. Conlin, A.P. McCartney, and N. Gibson. ENDFtk. https://github.com/njoy/ENDFtk/, 2020.

[ICS19] International Handbook of Evaluated Criticality Safety Benchmark Experiments/Nuclear Energy Agency. Technical Report (NEA;7328), Paris: OECD Nuclear Energy Agency, 2019.

[KDO+20] K. J. Kelly, M. Devlin, J. M. O'Donnell, J. A. Gomez, D. Neudecker, R. C. Haight, T. N. Taddeucci, S. M. Mosby, H. Y. Lee, C. Y. Wu, R. Henderson, P. Talou, T. Kawano, A. E. Lovell, M. C. White, J. L. Ullmann, N. Fotiades, J. Henderson, and M. Q. Buckner. Measurement of the ^{239}Pu(n, f) prompt fission neutron spectrum from 10 kev to 10 mev induced by neutrons of energy 1–20 mev. *Phys. Rev. C*, 102:034615, Sep 2020.

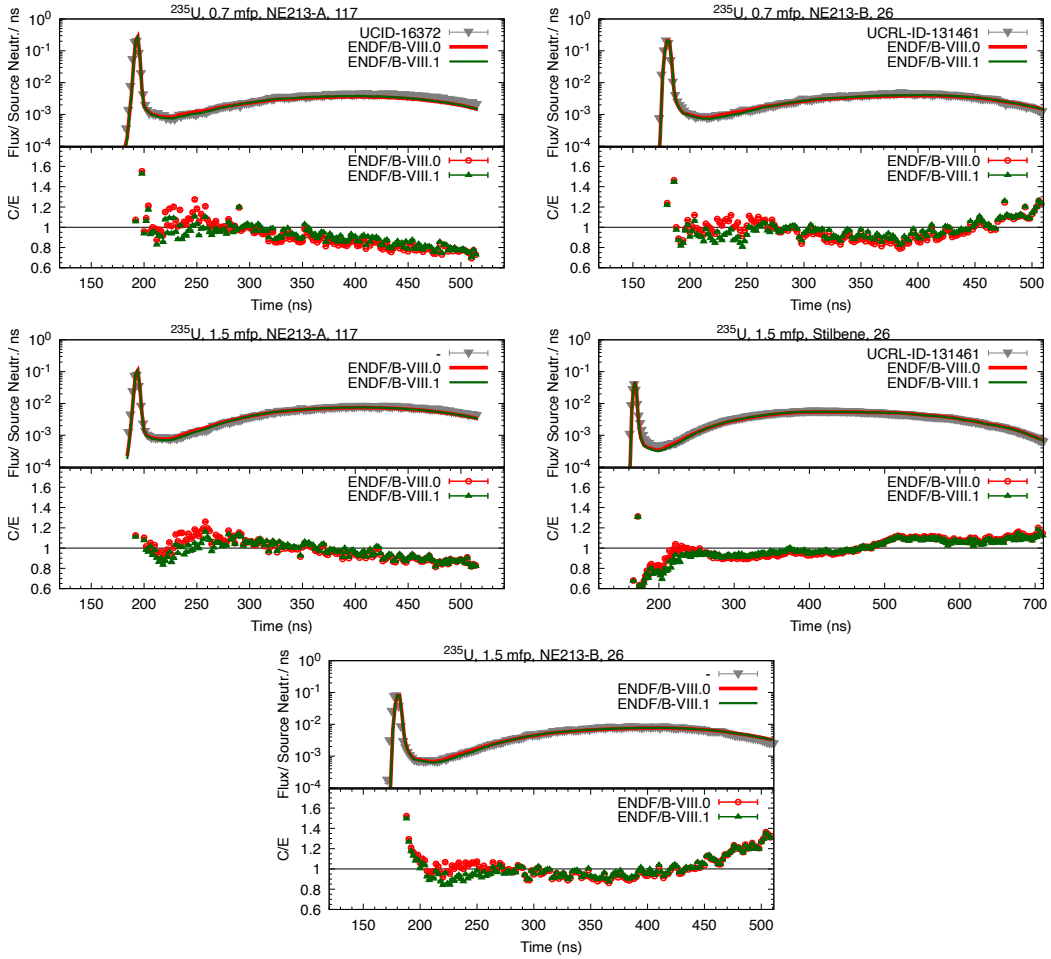

Figure 23: LLNL pulsed-sphere neutron-leakage spectra simulated with ENDF/B-VIII.0 and ENDF/B-VIII.1β1 for ^{235}U compared to experimental data.

[KGD+22] K. J. Kelly, J. A. Gomez, M. Devlin, J. M. O'Donnell, D. Neudecker, A. E. Lovell, R. C. Haight, C. Y. Wu, R. Henderson, T. Kawano, E. A. Bennett, S. M. Mosby, J. L. Ullmann, N. Fotiades, J. Henderson, T. N. Taddeucci, H. Y. Lee, P. Talou, and M. C. White. Measurement of the ^{235}U(n, f) prompt fission neutron spectrum from 10 kev to 10 mev induced by neutrons of energy from 1 mev to 20 mev. *Phys. Rev. C*, 105:044615, Apr 2022.

[KMT+21] K.J. Kelly, P. Marini, J. Taieb, M. Devlin, D. Neudecker, R.C. Haight, G. Bélier, B. Laurent, P. Morfouace, J.M. O'Donnell, E. Bauge, M.B. Chadwick, A. Chatillon, D. Etasse, P. Talou, M.C. White, C.Y. Wu, and E.A. Bennett. Comparison of results from recent nnsa and cea measurements of the 239pu(n, f) prompt fission neutron spectrum. *Nuclear Data Sheets*, 173:42–53, 2021. Special Issue on Nuclear Reaction Data.

[LNCea23] A.M. Lewis, D. Neudecker, A.D. Carlson, and et al. Templates of expected measurement uncertainties for capture and charged-particle production cross section observables. *Europ. Phys. J. N*, submitted, 2023.

[LNT22] A.E. Lovell, D. Neudecker, and P. Talou. Release of evaluated ^{235}u(n,f) average prompt fission neutron multiplicities including the cgmf model. Technical Report LA-UR-22-23475, Los Alamos National Laboratory, 2022.

[LS14] J.P. Lestone and E.F. Shores. Uranium and Plutonium Average Prompt-fission Neutron Energy Spectra (PFNS) from the Analysis of NTS NUEX Data. *Nuclear Data Sheets*, 119:213–216, 2014.

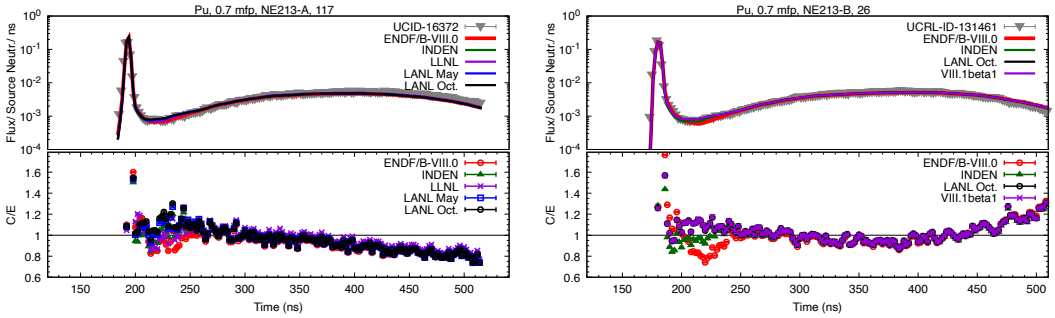

Figure 24: LLNL pulsed-sphere neutron-leakage spectra simulated with ENDF/B-VIII.0 and ENDF/B-VIII.1β1 for Pu compared to experimental data.

[Mat20] E.F. Matthews. *Uncertainty Analysis Procedures for Neutron-Induced Cross Section Measurements and Evaluations.* PhD thesis, Department of Nucl. Engineering, University of California, Berkeley, 2020.

[Mat21] E.F. Matthews. *Advancements in the Nuclear Data of Fission Yields.* PhD thesis, Department of Nucl. Engineering, University of California, Berkeley, 2021.

[Mea23] E.F. Matthews and et al. Templates of expected measurement uncertainties for fission yields. *Europ. Phys. J. N*, submitted, 2023.

[MMB+17] R.E. MacFarlane, D.W. Muir, R.M. Boicourt, A.C. Kahler, J.L. Conlin, and W. Haeck. The NJOY Nuclear Data Processing System, Version 2016. Technical Report LA-UR-17-20093, Los Alamos National Laboratory, 2017.

[MR13] W.J. Marshall and B.T. Rearden. The scale verified archived library of inputs and data - valid. Technical report, Proceedings of NCSD 2013: Criticality Safety in the Modern Era - Raising the Bar, Wilmington, NC, 2013.

[MTL+20] P. Marini, J. Taieb, B. Laurent, G. Belier, A. Chatillon, D. Etasse, P. Morfouace, M. Devlin, J. A. Gomez, R. C. Haight, K. J. Kelly, J. M. O'Donnell, and K. T. Schmitt. Prompt-fission-neutron spectra in the ^{239}Pu(n, f) reaction. *Phys. Rev. C*, 101:044614, Apr 2020.

[MTN+21] P. Marini, J. Taieb, D. Neudecker, G. Bélier, A. Chatillon, D. Etasse, B. Laurent, P. Morfouace, B. Morillon, M. Devlin, J. A. Gomez, R. C. Haight, K. J. Kelly, and J. M. O'Donnell. Energy dependence of prompt fission neutron multiplicity in the ^{239}pu(n, f) reaction, 2021.

[NCC+21] D. Neudecker, O. Cabellos, A.R. Clark, W. Haeck, R. Capote, A. Trkov, Morgan C. White, and Michael E. Rising. Which nuclear data can be validated with llnl pulsed-sphere experiments? *Ann. Nucl. Energy*, 159:108345, 2021.

[NCCea23] D. Neudecker, A.D. Carlson, S. Croft, and et al. Templates of expected measurement uncertainties for average prompt and total fission neutron multiplicities. *Europ. Phys. J. N*, submitted, 2023.

[NDHea23] D. Neudecker, M. Devlin, R.C. Haight, and et al. Templates of expected measurement uncertainties for prompt fission neutron spectra. *Europ. Phys. J. N*, submitted, 2023.

[Neu21a] D. Neudecker. Definitions for testing whether evaluated nuclear data relative uncertainties are realistic in size. Technical Report LA-UR-21-32171, Los Alamos National Laboratory, 2021.

[Neu21b] D. Neudecker. To adjust or not to adjust–a csewg discussion point for decades! Technical Report LA-UR-21-28012, Los Alamos National Laboratory, 2021.

[Neu22] D. Neudecker. Test Results for Checking Reliability of Selected ENDF/B-VIII.0 Evaluated Uncertainties. Technical Report LA-UR-22-21551, Los Alamos National Laboratory, 2022.

[NGA+23] Neudecker, D., Grosskopf, M.J., Alwin, J., Cutler, T., Frankle, S., Gibson, N., Haeck, W., Herman, M.W., Hutchinson, J., Kleedtke, N., Michaud, I.J., Rising, M.E., Smith, T., Thompson, N., and Vander Wiel, S. Understanding the impact of nuclear-data covariances on various integral responses using adjustment. *EPJ Web Conf.*, 281:00007, 2023.

[NHT+18] Neudecker, Denise, Hejnal, Brooke, Tovesson, Fredrik, White, Morgan C., Smith, Donald L., Vaughan, Diane, and Capote, R. Template for estimating uncertainties of measured neutron-induced fission cross-sections. *EPJ Nuclear Sci. Technol.*, 4:21, 2018.

[NK22] Denise Neudecker and Keegan John Kelly. Including chi-nu ^{235}u pfns experimental data into an endf/b-viii. 1 release candidate evaluation. Technical Report LA-UR-22-22220, Los Alamos National Laboratory, 2022.

[NKM22] D. Neudecker, K.J. Kelly, and P. Marini. Release of Evaluated ^{239}Pu(n,f) Prompt Fission Neutron Spectra Including the CEA and Chi-Nu High-precision Experimental Data. Technical Report LA-UR-22-23754, Los Alamos National Laboratory, 2022.

[NLK+23] D. Neudecker, A. E. Lovell, K. J. Kelly, P. Marini, L. Snyder, M. C. White, P. Talou, M. Devlin, J. Taieb, and M. B. Chadwick. Shedding light on the 239pu fission source term with new high-precision experiments and advanced fission modeling. *Frontiers in Physics*, 10, 2023.

[NLMea23] D. Neudecker, A.M. Lewis, E.F. Matthews, and et al. Templates of expected measurement uncertainties. *Europ. Phys. J. N*, submitted, 2023.

[NLT21] D. Neudecker, A.E. Lovell, and P. Talou. Producing endf/b-quality evaluations of ^{239}pu(n,f) and ^{235}u(n,f) average prompt neutron multiplicities using the cgmf model. Technical Report LA-UR-21-29906, Los Alamos National Laboratory, 2021.

[NPS21] Denise Neudecker, Vladimir G. Pronyaev, and Luke Snyder. Including 238u(n,f)/235u(n,f) and 239pu(n,f)/235u(n,f) niffte fission tpc cross-sections into the neutron data standards database. 6 2021.

[NST+20] D. Neudecker, D.L. Smith, F. Tovesson, R. Capote, M.C. White, N.S. Bowden, L. Snyder, A.D. Carlson, R.J. Casperson, V. Pronyaev, S. Sangiorgio, K.T. Schmitt, B. Seilhan, N. Walsh, and W. Younes. Applying a template of expected uncertainties to updating 239pu(n,f) cross-section covariances in the neutron data standards database. *Nuclear Data Sheets*, 163:228–248, 2020.

[NTK+18] D. Neudecker, P. Talou, T. Kawano, A.C. Kahler, M.C. White, T.N. Taddeucci, R.C. Haight, B. Kiedrowski, J.M. O'Donnell, J.A. Gomez, K.J. Kelly, M. Devlin, and M.E. Rising. Evaluations of energy spectra of neutrons emitted promptly in neutron-induced fission of 235u and 239pu. *Nuclear Data Sheets*, 148:293–311, 2018. Special Issue on Nuclear Reaction Data.

[NWVS20] Neudecker, Denise, White, Morgan Curtis, Vaughan, Diane Elizabeth, and Srinivasan, Gowri. Validating nuclear data uncertainties obtained from a statistical analysis of experimental data with the "physical uncertainty bounds" method. *EPJ Nuclear Sci. Technol.*, 6:19, 2020.

[ODS+14] N. Otuka, E. Dupont, V. Semkova, B. Pritychenko, A.I. Blokhin, M. Aikawa, S. Babykina, M. Bossant, G. Chen, S. Dunaeva, R.A. Forrest, T. Fukahori, N. Furutachi, S. Ganesan, Z. Ge, O.O. Gritzay, M. Herman, S. Hlavač, K. Katō, B. Lalremruata, Y.O. Lee, A. Makinaga, K. Matsumoto, M. Mikhaylyukova, G. Pikulina, V.G. Pronyaev, A. Saxena, O. Schwerer, S.P. Simakov, N. Soppera, R. Suzuki, S. Takács, X. Tao, S. Taova, F. Tárkányi, V.V. Varlamov, J. Wang, S.C. Yang, V. Zerkin, and Y. Zhuang. Towards a more complete and accurate experimental nuclear reaction data library (exfor): International collaboration between nuclear reaction data centres (nrdc). *Nuclear Data Sheets*, 120:272–276, 2014.

[RBB+20] Catherine Romano, Lee Bernstein, Teresa Bailey, Friederike Bostelmann, David Brown, Yaron Danon, Robert Casperson, Jeremy Conlin, Matthew Devlin, Bethany Goldblum, Michael Grosskopf, Amanda Lewis, Denise Neudecker, Ellen O'Brien, Bruce Pierson, Brian Quiter, Andrew Ratkiewicz, Gregory Severin, Michael S. Smith, Vladimir Sobes, Alejandro Sonzogni, Patrick Talou, Fredrik Tovesson, Etienne Vermeulen, Kyle Wendt, and Michael Zerkle. Proceedings of the workshop for applied nuclear data: WANDA2020. *ORNL/TM-2020/1617*, 2020.

[RWJ+11] B.T. Rearden, M.L. Williams, M.A. Jessee, D.E. Mueller, and D.A. Wiarda. Sensitivity and uncertainty analysis capabilities and data in scale. *Nuclear Technology*, 174(2):236–288, 2011.

[SAB+21] L. Snyder, M. Anastasiou, N.S. Bowden, J. Bundgaard, R.J. Casperson, D.A. Cebra, T. Classen, D.H. Dongwi, N. Fotiades, J. Gearhart, V. Geppert-Kleinrath, U. Greife, C. Hagmann, M. Heffner, D. Hensle, D. Higgins, L.D. Isenhower, K. Kazkaz, A. Kemnitz, J. King, J.L. Klay, J. Latta, E. Leal-Cidoncha, W. Loveland, J.A. Magee, B. Manning, M.P. Mendenhall, M. Monterial, S. Mosby, D. Neudecker, C. Prokop, S. Sangiorgio, K.T. Schmitt, B. Seilhan, F. Tovesson, R.S. Towell, N. Walsh, T.S. Watson, L. Yao, and W. Younes. Measurement of the 239pu(n,f)/235u(n,f) cross-section ratio with the niffte fission time projection chamber. *Nuclear Data Sheets*, 178:1–40, 2021.

[Smi21] D.L. Smith. Guidance on Generating Neutron Reaction Data Covariances for the ENDF/B Library by the CSEWG Covariance Committee. https://www.nndc.bnl.gov/endfdocs/ENDF-378.pdf, 2021.

[TSJ+21] P. Talou, I. Stetcu, P. Jaffke, M.E. Rising, A.E. Lovell, and T. Kawano. Fission fragment decay simulations with the CGMF code. *Computer Physics Communications*, 269:108087, dec 2021.

[VHHea23] J.R. Vanhoy, R.C. Haight, S.F. Hick, and et al. Templates of expected measurement uncertainties for (n,xn) cross sections. *Europ. Phys. J. N*, submitted, 2023.

[WAB+72] C. Wong, J. Anderson, P. Brown, L. F. Hansen, J. L. Kammerdiener, C. Logan, and B. Pohl. Livermore pulsed sphere program: Program summary through july 1971. *LLNL UCRL-51144 Rev. 1*, 1972.

[Wag01] J.C. Wagner. Computational benchmark for estimation of reactivity margin from fission products and minor acitnides in pwr burnup credit. Technical Report NUREG/CR-6747, US Nuclear Regualtory Commission, Washington, DC, 2001.